STATUS REPORT ON NIMROD, THE 7 GeV PROTON SYNCHROTRON AT THE RUTHERFORD HIGH ENERGY LABORATORY*

P. Bowles, H. C. Brooks, P. D. Dunn, D. A. Gray, G. S. Grossart, L. C. W. Hobbis, J. C. Louth, L. B. Mullett

The Rutherford High Energy Laboratory, England

INTRODUCTION

The construction of Nimrod, the 7 GeV proton synchrotron at the Rutherford High Energy Laboratory, is now complete. We give here the more important performance details obtained so far with only such general description as is necessary for that purpose. References [1—7] are given to more complete descriptions. Construction of the machine was completed early in August this year, and a few times 10^9 particles were accelerated to an energy of 8 GeV on August 27th. Some optimisation resulted in a beam of 10^{10} particles per pulse at an energy of 7 GeV.

INJECTOR

The Nimrod Injector is designed to inject up to 10^{14} protons and should be capable of producing at least 20 mA for a maximum pulse length of 1.5 ms. This injection time corresponds to a lower limit of $\dot{B}$ of 2 kGs/s. Optimum injection conditions cannot be predicted but it is anticipated that they will be covered by the available range of parameters. The main parameters of the machine are summarised in Appendix 1.

The linac is a strong focussing Alvarez structure operating at 115 MHz and fed by an RF system designed to provide 1.5 MW pulses of 2.5 ms duration at a repetition rate of 2 per second maximum. It first accelerated protons to 15 MeV on 1st August, 1961. After a short initial period of operation considerable trouble from multipactor was encountered for several months. Neither the usual conditioning procedures nor the use of a very fast rise of power level in the anode circuit of the final power amplifier led to reliable breakthrough of the multipactor levels. A satisfactory solution was obtained by coating with lampblack those parts of the drift tube faces showing multipactor patterns. It is painted on using a suspension of lampblack in alcohol. Although used on all 49 gaps initially it was eventually left off the first ten since its presence led to excessive sparking difficulties in this region of the tank.

The RF power system used initially was a driven one with a Siemans RS1041 final amplifier feeding the tank. Reliable operation has however been obtained using this valve and the previous driver stage, an English Electric BW165, in series as a self oscillator system, an arrangement much to be preferred since it automatically eliminates the need for servo-tuning of the linac tank and obviates the difficulties introduced by reactive beam loading. A fast field level stabiliser loop is in use. RF coupling details are rather unusual; they are illustrated in Fig. 1. The whole RF

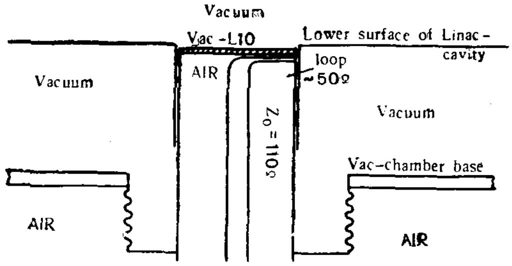

Fig. 1.

feed line is at atmospheric pressure and the large window diameter enables adequate coupling to be obtained without the loop having to penetrate beyond the liner surface. If such penetration were necessary a slightly domed window could be used.

On one occasion 16 mA currents have been obtained at 15 MeV without using the buncher and on another, 24 mA was obtained with

* The report was not read.

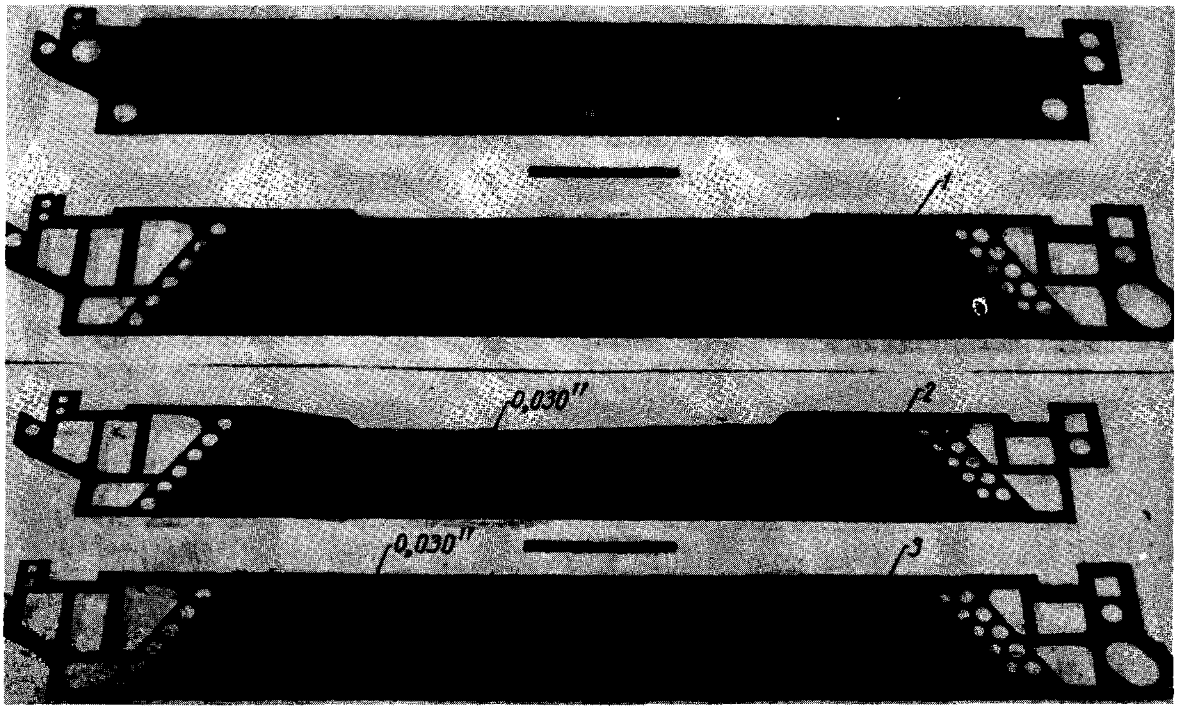

Fig. 2. Polepiece laminations:
1 — medium crenellation; *2* — deep crenellation; *3* — shallow crenellation; above — saturable fins.

the buncher operating, and a preinjector current of 42 mA. Transmission factors exceeding 0.6 have been found using the buncher. If optimum conditions (with improved ion sources) were available simultaneously we would expect to reach 30 mA, but the current will probably be limited to a lower figure by the maximum RF power available. Using the type of ion source developed at CERN by Schneider and Tallgren, 40 mA at 600 keV has been readily obtainable, but sparking in the extraction region limited source lifetime, sometimes severely. Recent work with a different design of RF source has eliminated this objection and the current at 600 keV may be improved to 100 mA or more in the near future. A duoplasmatron source is under investigation in parallel with further development of the RF source. The debuncher is installed in the high energy drift space but has not yet been commissioned. The achromatic inflector system has been used to inject a 15 mA beam into the magnet ring.

MAGNET

The C-magnet is fitted with pole pieces incorporating saturable fins [3] (Fig. 2). A correction is made of the shape of the field at high field values by means of crenellated inner shims. An intensive survey [4] of the magnetic field in the gap and some fringe fields has been made by energising half the magnet at any one time. By using four different arrangements of the magnet a complete survey was obtained while enabling construction work to continue on the un - energised half of the magnet.

The following characteristics were measured:

1. Field gradient (n-values) to an accuracy of 1%.
2. Magnetic median surface (B_p) to an accuracy of 0. 05 inch.
3. Comparison of effective length of pairs of octants to 0.02%.
4. Field values in the straight sections and in the radial fringe field of about 1%.

The pulsed measurements were converted to digital form and fed directly to a 7090 computer which carried out the appropriate integration. The results [5] have been used to prepare the programmes for pole face windings.

The Nimrod proton extraction system requires a Piccioni target, a plunged quadrupole and a plunged deflector magnet. A digitally servo-controlled hydraulic ram system will be used for the plunging. The quadrupole and magnet have been surveyed magnetically and the magnet is installed in the machine. The plunging mechanisms are being developed and have plunged so far at only slow rates. A fast kicker coil for bubble chamber beams (about 50 μs long) has been energised in the laboratory and shown to give the desired fields.

MAGNET POWER SUPPLY

The Nimrod magnet power supply [6] consists of two motor-alternator-flywheel sets which power the magnet via phase splitting transformers and ninety-six single anode water cooled steel tank mercury arc rectifiers. A 24 phase arrangement has been adopted. The alternators are 60 MVA, 12.8 kV machines, the flywheels each weigh 30 t and the drive motors of 5,000 HP each.

The equipment has now been operated as follows:

Total power supply running hours . . .	3,200
Total power supply pulsing hours	1,800
Total number of magnet pulses	1,500,000

The rotary plant weighs about 400 t and is mounted on a foundation block weighing about 1,200 t which is supported in turn on 80 spring units and twelve viscous damper units. The natural frequencies of the block are above those corresponding to the set running speed while those of the spring system are well below those corresponding to the normal set running speed, but are appreciably above the highest pulsing frequency. When the power plant is pulsing virtually no vibration is transmitted to nearby structures. When pulsing at 10,500 A magnet current the block movement is of the order $\pm 0.02''$. The foundation block profile changes quite rapidly with variation in temperature so that it has proved desirable to misalign the set when cold in order to achieve better operating conditions when hot.

The rotary plant is equipped with vibration and shaft eccentricity measuring equipment. The shaft system is also continuously monitored for excessive torsional stress and the mechanical monitoring is provided. Special ultrasonic flaw detection equipment [7] has been developed to inspect the forgings of motor rotors, alternator rotors and flywheel half shafts from a central bore hole. Bore surface flaws can be detected using surface wave probes while flaws in the body of the forging can be detected using longitudinal and/or transverse wave probes. The alternator automatic voltage regulation system has proved to be extremely accurate and capable of giving high reproducibility over long periods of pulsing.

For each half of the plant there are four main rectifier transformers each having a primary rating of 11.93 MVA and supplied at 12.8 kV from the alternators via an air blast circuit breaker. Each transformer has two secondary windings connected double star with interphase transformer, the no load secondary voltage being 3,400 V phase to neutral. The primary windings of the transformers are connected star; delta; extended delta $+15^\circ$ and extended delta -15° such that each half of the convertor plant operates as a 24 phase unit. The secondary windings of the transformer having the star connected primary are associated with convertor groups 1 and 2; the delta connected transformer with groups 3 and 4 and so on. Provision is made for reduced $\dot{B}$ at injection and also for a flat top slope control. Flat top duration can be 1 s for long pulse extraction. Ripple voltages will be reduced using a dynamic ripple filter system.

RF SYSTEM

The main frequency programme is derived from a signal from pick-up coils in the octants which is used to bias a ferrite permeability tuned Colpitts oscillator. The sequence is initiated by means of a signal from a peaking strip. This programme has a maximum deviation from the correct freguency of about 5%. A 20 point preset function generator provides a correcting signal over the frequency band. It is intended to provide a continuous correction by means of a signal from a pair of radial beam control electrodes. The low power RF system is transistorised throughout.

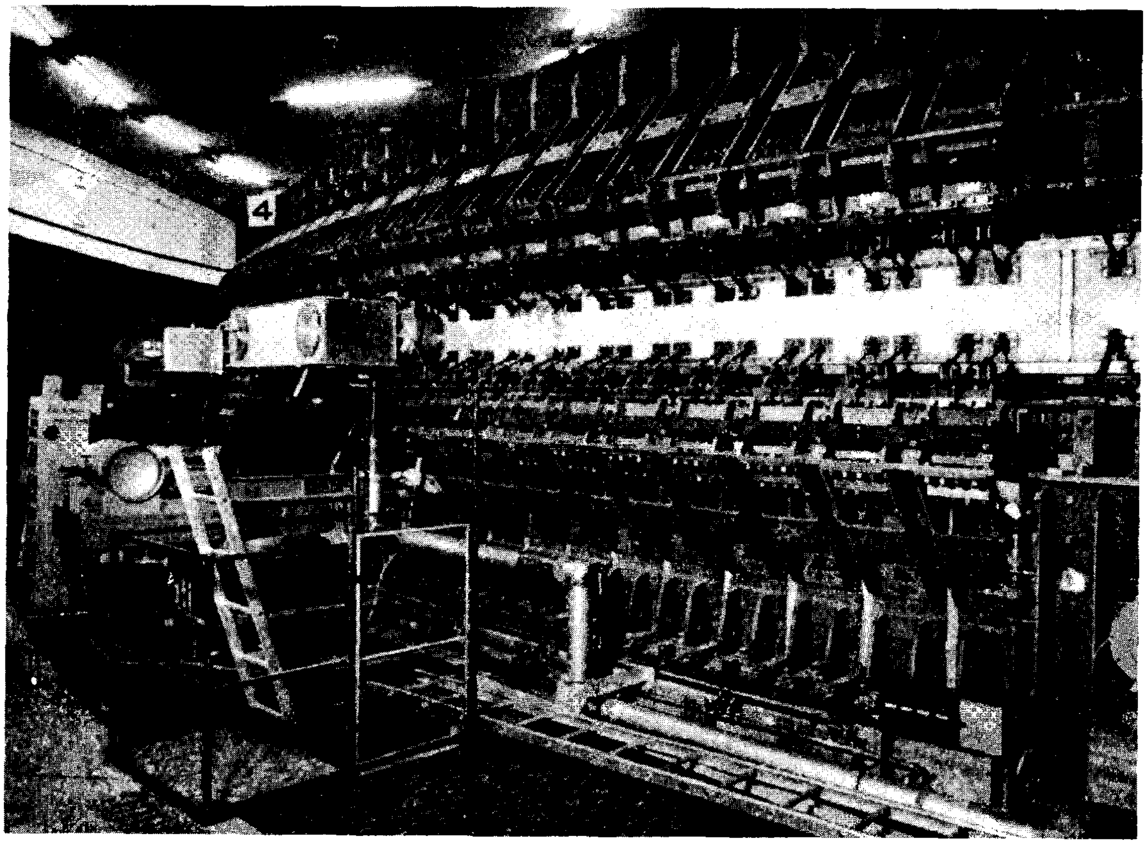

Fig. 3.

The cavity is magnetically screened by constructing the top, bottom, and side walls of 1" thick copper clad steel, and the end walls 1.5" of the same material. A two turn RF winding is used to raise the impedance presented to the amplifier. A 10-turn bias winding between the ferrite and cavity walls carries a peak current of 800 A and a peak voltage of 50 V.

The output stage of the drive chain consists of two water-cooled triodes in push-pull. Each have an anode dissipation of 30 kW, and are cross neutralised; the anodes are connected directly to the cavity. The output stage is driven by a broad-band driver, whose final stage is a cathode follower. This cathode follower is driven through a 1 : 1 coupling transformer (ferrite cored). Provision is made for automatic level control. Two bias supplies have been constructed: The Mk. I uses the Q Kerns circuit as in the Bevatron. The output rectifiers are germanium, the high voltage ones (10 kV) are selenium. The Mk. II supply. The circuit is a simple current amplifier, with an output stage of 192 transistors in parallel on a water-cooled heat sink.

BEAM DIAGNOSTIC EQUIPMENT

Injection conditions have been studied, with a beam of variable duration (0.3 μs upwards) using a chopper just after the injector. This beam was initially viewed by television on scintillators, a series of eight grids across the whole aperture which are viewed on one split-field screen. Eight movable targets whose positions are accurately controlled by a servo actuator system operated from the main control room are also available. Beam induction electrodes which will eventually be used in RF programming system are used to detect and measure spiralling chopped beams of less than 1 turn's length.

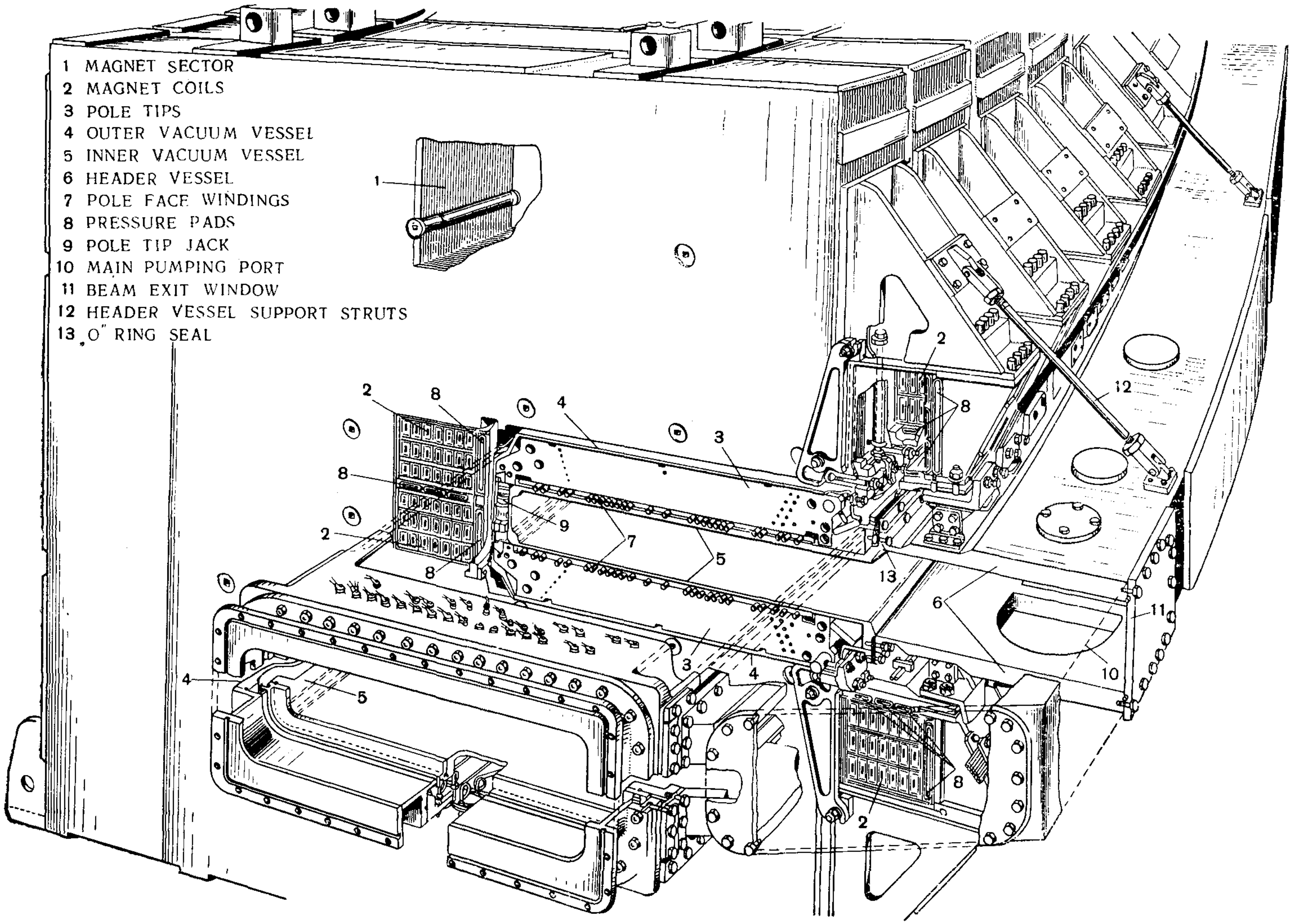

Fig. 4. Pictorial view of typical cross section through magnet octant of Nimrod.

VACUUM SYSTEM

The general arrangement of the epoxy-glass double walled vacuum vessel system is shown in Figs. 3,4. In the final machine assembly 4 of the octants from which beam extraction is not required, are fitted with polythene closure plates instead of header chambers.

All the vacuum vessels for the machine have been delivered and tested for vacuum tightness prior to installation. The difficulties encountered in manufacture were successfully overcome and techniques and materials developed which satisfactorily effected repairs to areas found to be leaking under test. The vessel performance is summarised in Table 1. An average pressure of down to 5×10^{-7} Torr has been achieved in the machine. If the vessel is let up to atmospheric pressure for periods of less than 48 h the pump down time 10^{-6} Torr is between 12 and 24 h. In order to determine the rate of degradation of the vacuum vessels due to radiation damage a programme of high level radiation dosimetry has been instituted.

Table 1

Vessel Number	Number of Leaks	Final Leak Rate 10^{-3} Torr	Installed in Octant Number
	Outer Vessel Proof Tests		
1	3	4.1	5
2	5	1.8	4
3	10	2.6	1
4	10	1.6	8
5	7	2.2	2
6	6	2.8	3
7	3	1.9	6
8	14	2.0	7
9	5	3.8	Spare
10	2	1.1	Spare
	Inner Vessel Proof Tests		
1	4	0.26	1
2	3	0.17	8
3	3	0.18	2
4	5	0.21	4
5	2	0.38	5
6	7	0.09	6
7	4	0.50	3
8	5	0.30	7
9	3	0.33	Spare
10	2	0.12	Spare
	Header Vessel Proof Tests *		
1	96	30 (approx)	Returned for Rectification
2	97	3.5	3
3	2	1.1	6
4	4	1.1	4
1	5	0.66	5

* Leak rate includes associated inner vessel leakage.

A system of graphite beam trimmers and screens, some of them water cooled, has been installed to reduce the risk of damage to the inner vacuum chamber by the injected beam, and to provide monitoring points for the beam loss. Thermistors have also been fixed inside the inner vessel.

Twelve additional 12″ pumping units are being provided to supplement the main system of forty 24″ Oil Diffusion Pumps. The latter units have all been tested and installed in the magnet room. Performance is well up to specification, speeds of over 3000 l/s at 10^{-6} Torr being commonly measured, together with ultimate pressures of 10^{-7} Torr (non-Alpert type gauge).

APPENDIX I. MACHINE PARAMETERS

Injector parameters

Ion Source

Extraction Potential . .	5—25 kV
Extraction Current . . .	25—100 mA
Pulse Length	50 μs—1.5 ms variable 0.3 μs and 5 μs fixed
Pulse repetition frequency	2 per sec. maximum

Pre-Injector

Focussing	Electrostatic
Energy	600 keV
Beam emittance (area/π)	Up to 5×10^{-3} cm·rad

Low Energy Drift Space

Focussing	
First triplet	8.9 cm aperture max. gradient 170 Gs/cm
Second triplet . . .	7.6 cm aperture max. gradient 240 Gs/cm
Third triplet	6.4 cm aperture max. gradient 480 Gs/cm
Peak RF voltage on buncher gap	23 kV maximum
Buncher Q	≈1500 with external resistive loading
Buncher drift length . .	1.4 m
Bunching factor (measured)	2.2
Plateau width (theoretical)	6 keV

Linac

Frequency	115 MHz
Beam current	10 mA with buncher
Acceptance (area/π) (+—+—, theoretical) . . .	3.0×10^{-2} cm·rad at 600 keV
Synchronous phase . . .	30°
RF Pulse Length . . .	2.5 ms

Pulse repetition frequency	2 per sec. max
Quadrupole Gradients	
First drift-tubes	3,700 Gs/cm
Last drift-tube	640 Gs/cm
Tank length	13.45 m
Tank diameter (effective)	1.69 m
Drift-tube diameter	28.2 cm
Input aperture	2.1 cm
Output aperture	5.0 cm
Output energy	14.9 MeV
Resonator Q (measured)	80,000
RF power at Q=80,000 (theoretical)	800 kW
Peak RF voltage on input gap	140 kV
Peak RF voltage on output gap	680 kV
Energy spread (total)	300 keV
Operating temperature	20° C

High Energy Drift Space

Focussing	
First triplet	7.6 cm aperture max. gradient 730 Gs/cm
Second triplet, Third triplet, Fourth triplet	8.9 cm aperture max. gradient 430 Gs/cm
Peak RF voltage on de-buncher gap	240 kV
De-buncher Q (measured)	20,000
De-buncher drift length	10.7 m

Achromatic Inflector System

Achromatic mode	Single Crossover
Total deflection	+25°
Number of elements	5

Angle	Radius of Central Orbit, m	Apertures Radial, cm	Apertures Vertical, cm
'C' magnet —25°	0.7	6	9
'C' magnet +50°	0.7	6	9
'C' magnet —36.5°	0.7	6	9
Shielded 'C' magnet +26°	1.124	5	8
Electrostatic element +10.5°	6.0	3	8

Vacuum System

Location	Number of Pumps	Size	Working Pressure Range (mm Hg)
DC Gun	2 (Mercury)	9″	3×10^{-6}
Buncher	1 (Mercury)	9″	1×10^{-6}
Linac	Up to 4 (Mercury)	24″	$1—2\times10^{-6}$
Beam Chopper	1 (Ion Pump)		
HEDS	2 (Mercury)	6″	$1—5\times10^{-6}$
De-buncher	1 (Mercury)	9″	$1—5\times10^{-6}$
Achromatic inflector system	2 (Ion Pumps)		

RF System

(The following data assumes an initial $\dot{B}$ of 0.3 Wb/m²·s, rising in 10 ms to a steady value of 2.0 Wb/m²s)

Orbital frequency at injection (14.9 MeV)	355.6 kHz
at 7 GeV	2.003 MHz
Harmonic Number	4
Synchronous phase angle	30°
Energy gain per turn at 0.3 Wb/m²·s	837 eV
at 2.0 Wb/m²·s	5.58 keV
RF frequency error for 1 cm shift of closed orbit at injection	~450 Hz
Potential well depth at injection, 0.3 Wb/m²·s	51.5 keV
at 7 GeV, 2.0 Wb/m²·s	1.55 MeV
Energy Spread at 7 GeV, assuming W. K. B. approximation	1.01 MeV
Phase oscillation frequency at injection	2.004 kHz
at 7 GeV	2.496 kHz
Radial synchrotron amplitude at injection	8.11 cm
Max. stable synchrotron amplitude at 7 GeV	0.92 cm
Damped synchrotron amplitude at 7 GeV (W. K. B. approximation)	0.64 cm
Radial betatron amplitude at 7 GeV	7.32 cm
Accelerating Cavity Q at injection	10
at 7 GeV	40
Mean cavity power during pulse	~35 kW
Beam loading on cavity, at 10^{12} protons per pulse, 7 GeV	1.6 kW
Ferrite properties at 1.4 MHz	μ=600, Q=10 } BRF=60 Gs
biased to 8 MHz	Q=40
bias field	=12 ats/cm
Total ferrite wt.	= 6 t
Cavity Impedance at 1.4 MHz	3000 Ω
at 4.5 MHz	2000 Ω
at 8.0 MHz	8000 Ω
Beam electrode sensitivity	±1% at 10^9 protons per pulse; ±10% at 10^8 protons per pulse; 12.5 V at 10^{12} protons per pulse

Magnet and power supply

Magnet sector radius, R_0	18.781 m
Proton kinetic energy for B_0 = =10 кGs	4.77 GeV
for B_0=14 кGs	7.00 GeV
for B_0=15.8 кGs	8.00 GeV
Total straight section length (design)	30.480 m
Mean orbit radius, R_m	23.633 m
Number of straight sections	8 (4 long, 4 short)
Design length of long straights (each)	4.267 m

Design length of short straights (each)	3.353 m
Magnetic field index (design)	0.60
Magnetic length of octant at R_0 (design)	14.751 m
Total number of magnet yoke blocks	336
Number of pairs of polepieces per octant Mk I	28 (at centre of octant)
Number of pairs of polepieces per octant Mk II	12 (6 each side of Mk I's)
Number of pairs of polepieces per octant end	2
Number of yoke blocks per octant	42
Thickness of a yoke block (at R_0)	12.50″ (max)
Angle between centre lines of adjacent blocks	1.074°
Block-Block spacing at R_0	13.859″
Block-Block spacing at Front edges	14.253″
Block-Block spacing at Back edges	12.202″
Thickness of block at back edge	12.10″ (max)
Front edges of sectors lie on sector radius	19.355 m
Weight of yoke block	19.5 t
Total number of laminations per block	~47
Steel silicon content %	0.80 min 1.00 max
Vertical yoke gap	23.000″

Polepieces

Total number of laminations	450 approx.
Thickness of laminations—thin	0.020″ nominal
» » » —thick	0.030″ nominal
Ratio of number of thin to number of thick	1 : 2
Silicon content of thin lamination	3.5%
Silicon content of thick lamination	1.0%
Outside edge of magnetic profile of polepiece lies on a sector radius	63′7.9″
Radial length of magnetic profile of polepiece	45.5″
Vertical height of polepieces at R_0	5.875″
Number of coil turns	42
Total copper cross-section	~155 sq. ins.
Length of mean turn on an octant	~117 ft.
Total weight of copper	~250 t
Coil resistance (at 50° C)	0.108 Ω
Magnet inductance (low currents)	1.1 H

Magnet performance under standard pulse conditions

Peak current	9150 A
Rise time	0.72 s
Duration of flat-top	0.115 s
Current decay time	0.80 s
Repetition rate	26 per min
Mean voltage during rise	13.9 kV
Assumed voltage variation during ring rise	16.0 to 11.8 kV
Mean voltage during decay	—11.7 kV
Assumed voltage variation during decay	—11.0 to—13.4 kV
R.M.S. current	4550 A
VI at top of current rise	108 MW
VI during flat-top	9.1 MW
Energy delivered to magnet during a current rise:	
Stored energy	39 MJ
Copper loss	1.92 MJ
Eddy current loss	0.07 MJ
Energy delivered during flat-top	1.04 MJ
Energy required during current decay:	
Stored energy	39 MJ
Copper loss	2.03 MJ
Eddy current loss	0.08 MJ
Iron loss (hysteresis)	0.12 MJ
Net energy loss/pulse	5.26 MJ
Overall average losses	2.22 MW

Measured characteristics

Field versus current

Current, A	Field, kGs	Energy, GeV
2000	3.7	1.4
3000	5.6	2.4
4000	7.4	3.4
5000	9.3	4.4
6000	10.7	5.2
7000	12.1	5.9
8000	13.4	6.7
9150	14.6	7.3
10500	15.6	7.9

Estimated good field region using correction windings

B, gauss	Inner radius, inches	Outer radius, inches	Extent of good field, inches
300	723.2	758.2	36
600	724.2	758.2	34
2000	724.9	750.2	25.3
5000	731.2	748.7	17.5
7000	732.4	748.2	15.8
10000	733.4	747.4	14.0
12000	732.9	747.4	14.5
13000	732.9	747.7	14.8
14000	732.9	747.4	14.5
15000	732.9	746.7	13.8

REFERENCES

1. Nimrod (Design, Construction, Installation and Commissioning) Part 1, NIRL/R/44, 1956—December, 1962.
2. West N. D. Investigation of Energy Spread in the Beam from the Nimrod Injector Linac, NIRL/M/46.
3. Wilkins J. J. and Gray D. A. The Nimrod Magnet: Saturable-Fin Polepieces. NIRL/R/33.
4. Gray D. A., Harold M. R., Jones P. F., Morgan R. H. C., Partington J. E. and Pyle I. C. Measuring Appara-

tus and Methods used during the Design and Commissioning of Nimrod Magnet. NIRL/R/4.
5. Gray D. A., Harold M. R. and Morgan R. H. C. Some Nimrod Magnetic Survey Results. NDN 100/10.
6. Magnet Power Supply for Nimrod. Proc. I. E. E., March 1961. Pt. I. General. Bowles P., Hadley H., Marchbanks M. J., Wilkins J. J. Pt. 2. Rotating Machines. Fox J. A., Taylor D. G., Wilson R. Pt. 3. Mercury Arc Convertors. Rohlig K., Hödle H.
7. Ultrasonic Inspection of the Nimrod Power Plant Alternator Rotors. In: Proceedings of the 4th International Conference on Non Destructive Testing, paper 29, September, 1963.